# Sliding Orbits and Their Bifurcations in Relay Feedback Systems

Mario di Bernardo(*), Karl Johansson(+), Francesco Vasca(o)

(*) Department of Engineering Mathematics
University of Bristol, Bristol BS8 1AD, U.K.
Fax:+44-117-9251154, E-mail M.diBernardo@bristol.ac.uk

(+) Dept. of Electrical Eng. and Computer Sciences
UC Berkeley, 333 Cory Hall #1770, Berkeley, CA 94720-1770, U.S.A.
johans@eecs.berkeley.edu

(o) Università degli Studi del Sannio
Facoltà di Ingegneria, Corso Garibaldi 107
82100 Benevento, Italy

**Abstract**

This paper is concerned with the analysis of periodic solutions and their bifurcations in relay feedback systems. The occurrence of periodic solutions characterised by sliding sections is outlined and particular care is taken in studying the bifurcation leading to their formation. Discrete-time mappings are introduced and used to characterise the regions of existence and stability of various periodic orbits. Also, bifurcations of sliding orbits into more complex solutions such as multi-sliding orbits are investigated.

## 1 Introduction

The past few years have seen a dramatic increase of interest in the study of piecewise linear (PWL) systems in both the academic and industrial world. PWL models are used in many different branches of applied science [22, 10, 15, 16, 23, 9, 8]. In control engineering, for instance, the particular class of PWL systems referred to as relay feedback systems is well established and has many applications [14, 3]. Oscillators based on relay feedback have been particularly well studied [1, 4, 24].

From a geometric point of view, the phase space of a PWL system can be divided into countably many regions. The vector field in each region is defined by a linear differential equation. At the boundaries between the regions, the trajectory of the system is continuous, but may have

discontinuous time derivative. The trajectory of a PWL system therefore consists of sections lying in different regions of the phase space and the system is switching between different configurations whenever one of the boundaries is being crossed. A novel type of bifurcation, termed border-collision, has been suggested to occur when a section of a system trajectory becomes tangent to one of these boundaries as one or more system parameters are varied [21, 11, 12]. Border-collision bifurcations give rise to seemingly exotic dynamical transitions, which are unique to PWL systems. An example of these is sudden transition from a periodic attractor to a chaotic attractor.

It is well known that PWL systems can exhibit a peculiar type of solution, termed sliding motion [13, 25]. The sliding solution belongs to one of the boundaries that define the discontinuous change in the vector field and is a convenient mathematical construction that is motivated from modeling simplifications of real switching dynamics. For example, assume that the real switching for a system that the PWL model is supposed to represent takes some time $\epsilon > 0$. Then, for certain system parameters there exist solutions with switching period $2\epsilon$. As $\epsilon$ tends to zero, the solution converges to a solution that belongs to the boundary of the PWL system with a perfect switch. We can think of such a solution to have infinitely many switchings. For many different type of switching imperfections, the time relaxation described above being only one, it has been shown that the solution concepts by Filippov and Utkin agree with the limiting solution for a large class of systems. Let $S$ denote a hyperplane that defines the boundary between two regions. Then, in order to have sliding, the vector field on each side of $S$ must be pointing towards $S$ itself. Therefore, according to the direction of the vector fields close to $S$, it is possible to identify *sliding regions* on $S$ where sliding can occur. It can be shown that the dynamics of the PWL system within such a sliding region are given by a reduced order linear system. This dynamics can be obtained by applying Utkin's equivalent control method [25] or Filippov's convex method [13]. For PWL systems, these two methods agree.

In recent work by the authors, the existence of periodic solutions with sliding sections (termed *sliding orbits*) has been pointed out in the context of relay feedback systems [17, 18] and some power electronic devices [15, 9, 6]. The main contribution of this paper is an analytical and numerical study of the occurrence of this novel class of periodic solutions and their bifurcations in relay feedback systems. Particularly, the bifurcation of a non-sliding limit cycle into a limit cycle with sliding is described. First, however, the equations for the relay feedback system is recalled (§2). An analytical method, similar to the one reported in [2, 18], is outlined in order to study stability and existence of the periodic solutions (§3). Then the occurrence of periodic solutions with sliding motion is briefly discussed (§4), and bifurcations of non-sliding orbits into sliding ones are presented (§5). For further parameter variations, sliding orbits will be shown to bifurcate into more complex periodic solutions, termed *multi-sliding* orbits, characterised by more that one sliding section (§6). Finally, some comments about chattering orbits are given (§**??**).

It is relevant to point out that the analysis presented here can be applied, without major modifications, to other systems of relevance in engineering where sliding solutions have been

shown to play an important role in organising the system dynamics such as friction oscillators [23], DC/DC power converters [9, 7, 6] and many other [19]. During the preparation of this work, we have become aware of some preliminary results on the existence of sliding bifurcations, which were independently reported in the Russian literature [20].

## 2 Relay Feedback System

We consider a linear system with relay feedback given by

$$\dot{x} = Ax + Bu \tag{1}$$

$$y = Cx \tag{2}$$

$$u = -\operatorname{sign} y, \tag{3}$$

where $\operatorname{sign} y = 1$ if $y > 0$, $\operatorname{sign} y = -1$ if $y < 0$, and $\operatorname{sign} y \in [-1, 1]$ if $y = 0$. The relay feedback system is hence interpreted as a differential inclusion. A solution to (1)–() is an absolutely continuous function $x$ that satisfies this differential inclusion. Formal definitions for solutions in PWL systems follows as a special case from the definitions in [13, 25].

The bifurcation analysis and the examples in this paper refers to third-order dynamics given by

$$A = \begin{pmatrix} -(2\zeta\omega + \lambda) & 1 & 0 \\ -(2\zeta\omega + \omega^2) & 0 & 1 \\ -\lambda\omega^2 & 0 & 0 \end{pmatrix}, \quad B = \begin{pmatrix} k \\ 2k\sigma\rho \\ k\rho^2 \end{pmatrix}, \quad C = \begin{pmatrix} 1 \\ 0 \\ 0 \end{pmatrix}^T, \tag{4}$$

where $k > 0$ and $\lambda > 0$. This corresponds to the transfer function

$$G(s) = C(sI - A)^{-1}B = k\frac{(s^2 + 2\sigma\rho s + \rho^2)}{(s^2 + 2\zeta\omega s + \omega^2)(s + \lambda)}. \tag{5}$$

The switching plane is given by $S = \{x \in R^3 : Cx = 0\} = \{x \in R^3 : x_1 = 0\}$.

A relay feedback system, as the one described above, can exhibit several types of periodic solutions. As mentioned in the introduction, it has been shown that system (2) can exhibit periodic solutions characterised by sliding sections. In particular, we will term *non-sliding orbits* those orbits that have no sliding sections in $S$ and *sliding orbits* will indicate periodic solutions partially lying in $S$. Both these periodic solutions can be studied by imposing appropriate constraints on the system Poincaré maps [2, 17, 18]. In next section we describe in detail how the Poincaré map for the non-sliding orbit is derived and how it can be used to state conditions for existence and stability of non-sliding orbits. It is straightforward to modify this analysis for sliding orbits.

## 3 Non-Sliding Orbits

The dynamical behaviour of system (1) can be investigated by defining a Poincaré map describing the system dynamics from one intersection with the switching plane, $S$, to the next. In general, a

distinction needs to be made between system trajectories with sliding and those without sliding. In what follows, we will detail the derivation of the Poincaré map in the case of trajectories that do not have sliding. The map when sliding occurs can be derived similarly by considering the occurrence of sliding motion (see comments in next section).

### 3.1 Poincaré map

Let us consider a trajectory of the relay feedback system (1)–(2) characterised by intersecting the switching plane $S$ for $t = t_n$ at a point $x_n = [0, z_1, z_2]^T$ located outside the sliding strip. In this case, there will be no sliding motion on $S$ and the relay will switch to a new configuration, say $u = -1$. The system, then, will evolve in this phase until for $t = \tilde{t} > t_n$, the trajectory eventually hits the switching plane again at a point $\tilde{x}_n = [0, \tilde{z}_1, \tilde{z}_2]^T$. At this point the system switches back to the next phase, $u = +1$, and will evolve in this configuration until for $t = t_{n+1} > \tilde{t}$, the trajectory will intersect again the switching plane at a point $x_{n+1} = [0, z_1', z_2']^T$ etc.

A Poincaré map from the switching plane to itself

$$\Pi : (t_n, x_n) \mapsto (t_{n+1}, x_{n+1})$$

can be easily constructed. Specifically, given a generic initial condition in the switching plane, say $x_0 = x(0) \in S$, the solution will depending on the second component of $x_0$ be either

$$x(t) = N(t)x_0 - M(t) \tag{6}$$

for $u = -1$, or

$$x(t) = N(t)x_0 + M(t) \tag{7}$$

for $u = +1$, where $N(t) = \exp(At)$ and $M(t) = (N(t) - I)A^{-1}B$, assuming that $A$ is nonsingular. Therefore, starting from $(t_n, x_n)$, by using (6), the state at the successive switching can be written as

$$\tilde{x}_n = N(\delta_{n_1})x_n - M(\delta_{n_1}), \tag{8}$$

where $\delta_{n_1}$ is the time interval from $t_n$ to the next switching time instant, i.e., $\tilde{x}_n = x(t_n + \delta_{n_1})$. The time variable $\delta_{n_1}$ is implicitly defined by the following switching condition:

$$C\tilde{x}_n = C\left[N(\delta_{n_1})x_n - M(\delta_{n_1})\right] = 0. \tag{9}$$

After $t = t_n + \delta_{n_1}$ the system will evolve on the other side of the switching plane, i.e., the output will become negative and the input will be $u = 1$. The state at the next switching time instant $x_{n+1} = x(t_{n+1})$ will then be given by

$$x_{n+1} = N(\delta_{n_2})\tilde{x}_n + M(\delta_{n_2}) \tag{10}$$

where $t_{n+1} = t_n + \delta_{n_1} + \delta_{n_2}$ and $\delta_{n_2}$ is implicitly defined by the following switching condition:

$$Cx_{n+1} = C\left[N(\delta_{n_2})N(\delta_{n_1})x_n - N(\delta_{n_2})M(\delta_{n_1}) + M(\delta_{n_2})\right] = 0. \tag{11}$$

The Poincaré map can be obtained by substituting (8) in (10), thus providing

$$x_{n+1} = N(\delta_{n_2})N(\delta_{n_1})x_n - N(\delta_{n_2})M(\delta_{n_1}) + M(\delta_{n_2}), \tag{12}$$

where $\delta_{n_1}$ and $\delta_{n_2}$ are implicitly defined by (9) and (11).

### 3.2 Necessary conditions of existence

Necessary conditions can be given for the existence of periodic solutions. It is simple to show that the equilibrium point of the Poincaré map (12) can be written as

$$\bar{x} = \left[I - N(2\bar{\delta})\right]^{-1} \left[I - N(\bar{\delta})\right] M(\bar{\delta}), \tag{13}$$

where we assumed that the orbit is symmetric, i.e., $\delta_{n_1} = \delta_{n_2} = \bar{\delta}$. A necessary condition for the existence of such a periodic solution is given by (9) at steady state, i.e., by the scalar equation

$$C\left[N(\bar{\delta})\left(I - N(2\bar{\delta})\right)^{-1}\left(I - N(\bar{\delta})\right)M(\bar{\delta}) - M(\bar{\delta})\right] = 0. \tag{14}$$

By solving (14) we obtain candidate time intervals $\bar{\delta}$ (and the corresponding fixed points from (13)) for possible limit cycles. Once a candidate $\bar{\delta}$ have been obtained, the existence of the corresponding orbits and their stability must be verified.

### 3.3 Local stability

To investigate the stability of the periodic solutions located using the conditions outlined in the previous section, we now illustrate the derivation of the Jacobian of the Poincaré map around an equilibrium point corresponding to a given periodic solution.

Introducing the vector $\Delta_n = (\delta_{n_1}, \delta_{n_2})^T$, map (12) can be rewritten as follows:

$$x_{n+1} = f(x_n, \Delta_n) \tag{15}$$

and the switching conditions (9) and (11) can be rewritten in vector form as

$$\mu(x_n, \Delta_n) = 0. \tag{16}$$

By using implicit differentiation, the Jacobian can be computed as

$$J = \frac{df}{dx_n} = \frac{\partial f}{\partial x_n} - \frac{\partial f}{\partial \Delta_n}\left(\frac{\partial \mu}{\partial \Delta_n}\right)^{-1}\frac{\partial \mu}{\partial x_n}.$$

After some algebraic manipulation, we get

$$J = N_2 N_1 - \frac{1}{C\dot{\tilde{x}}_n^- C\dot{x}_{n+1}^-} N_1\left[\dot{\tilde{x}}_n^- C\dot{x}_{n+1}^- C + \dot{\tilde{x}}_n^+ C\left(\dot{\tilde{x}}_n^- C N_2 - N_2\dot{\tilde{x}}_n^- C\right)\right] N_1, \tag{17}$$

where $N_2 = N(\delta_{n_2})$, $N_1 = N(\delta_{n_1})$, $\dot{\tilde{x}}_n^- = A\tilde{x}_n - B$, $\dot{\tilde{x}}_n^+ = A\tilde{x}_n + B$, and $\dot{x}_{n+1}^- = Ax_{n+1} + B$. Note that the Jacobian is derived for the general case with asymmetric orbits. Eq. (17) can be used to check stability of symmetric orbits by assuming that $x_{n+1} = x_n = \bar{x}$ and $\delta_{n+1} = \delta_n = \bar{\delta}$ in (17) and then computing the eigenvalues of the corresponding Jacobian, cf. [2, 17, 18].

# 4 Sliding Orbits

Sliding motion is possible for the relay feedback system. Under sliding motion the system trajectory is constrained to lie on the switching hyperplane $S$. The equations of the reduced order system describing the system dynamics on $S$ are given by

$$\dot{z} = \begin{pmatrix} -2\sigma\rho & 1 \\ -\rho^2 & 0 \end{pmatrix} z, \tag{18}$$

where the state $z$ consists of the second and third components of $x$. Note that the eigenvalues of the system (18) are equal to the zeros of the transfer function (5). The origin is a stable equilibrium of (18) for $\sigma\rho > 0$ and unstable for $\sigma\rho < 0$.

In order to have sliding motion, the equivalent control [25] must satisfy the following constraint:

$$|u_{eq}| = \left|(CB)^{-1}CAx\right| < 1. \tag{19}$$

By substituting the system matrices (4) in (19), it is straightforward to see that (19) corresponds to $|x_2| < k$. Hence, the *sliding strip* is given by $-k < x_2 < k$.

The Poincaré map reported in the previous section is valid for non-sliding orbits. If we instead assume that, at a generic switching time $t_n$, the second component of $x_n$ is within the interval $(-k, k)$, then the trajectory will start sliding on the plane and the corresponding state evolution will be constrained to be within the sliding strip. If the sliding dynamics (18) is unstable, the trajectory will evolve towards the boundaries of the sliding strip. Hence, when the second component of $x$ (the first component of $z$) becomes equal to $\pm k$, the trajectory will "escape" from the switching plane and the corresponding state evolution will be described by (6) or (7).

It is possible to show that for some values of the system parameters a stable periodic trajectory is exhibited, which consists of four different parts: two sliding sections and two sections on either side of $S$ [18]. The Poincaré map of such an orbit can be obtained by following a similar procedure to that presented in the previous section by taking into account the onset of sliding dynamics described by (18). Specifically, let us indicate with $x_n$ the system state at a switching instant outside the sliding strip, and assume that from $x_n$ to $\tilde{x}_n$ (next intersection on $S$) the system undergoes a smooth evolution whose map can be described using (6). Assume that $\tilde{x}_n$ is in the sliding strip. In this case, a sliding motion will start whose dynamics can be described by solving (18). If the fixed point of the sliding equation (18) is unstable, the sliding state evolution will be then directed towards the border of the sliding strip. Let us indicate with $\bar{x}_n$ the state at which the border of the sliding strip is reached; the first component of $\bar{x}_n$ will be zero and its second component will be equal to $\pm k$. From $\bar{x}_n$, the system will then follow the evolution described by (7) and so on. The overall Poincaré map for a sliding orbit will therefore be the composition of two submappings: one describing the periodic connection and the other the sliding section of the orbit. These can be easily obtained by appropriately combining (6), (7), and the solution to (18).

Conditions for existence and local stability of the sliding orbit are readily derived by appropriately modifying the expression for the non-sliding orbit in the previous section.

## 5 Sliding Bifurcations

As shown above a relay feedback system can exhibit different types of periodic solutions, which can either contain sliding sections or not. In this section, we will seek to understand the mechanism behind the formation of sliding orbits and their further bifurcations, as the system parameters are varied. In doing so, we will vary the positions of the zeros of the transfer function (5), via variation of the parameter $\rho$. Hence, we will study the family of codimension-1 bifurcations resulting from this parameter variation. In next section we will instead vary the poles through the parameter $\omega$ and see that it gives bifurcations to multi-sliding orbits. The other parameters of (5) are fixed to $k = 1$, $\sigma = -1$, and $\lambda = 1$. The damping $\zeta = 1$ when $\rho$ is varied and $\zeta = 0.05$ when $\omega$ is varied. This means that $G$ has left half-plane poles and real right half-plane zeros. By varying $\rho$ and $\omega$, only the distances of the zeros and the poles to the origin is changed.

Careful numerical computation showed that as $\rho$ is varied, the system undergoes several bifurcations. These are summarised in the bifurcation diagram depicted in Fig. 1, where the second component of the Poincaré map is shown versus $\rho$. For decreasing values of $\rho$, we see

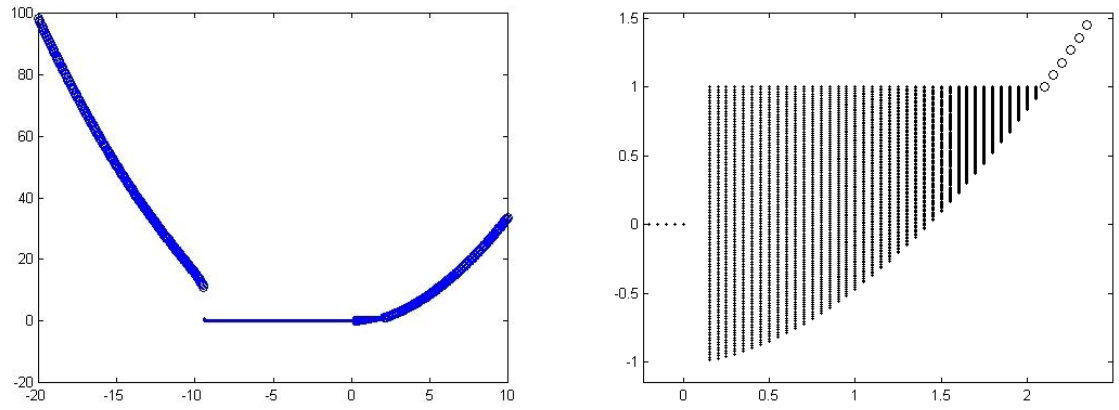


(a) (b)

Figure 1: Bifurcation diagram of system (2), when $\rho$ is varied. The second component of the Poincaré map is plotted against $\rho$ in (a). A zoom of the transition from simple to sliding orbit is shown in (b).

that a non-sliding orbit turns into a sliding orbit at $\rho \approx 2.1$. Then, for $\rho \in (-9.4, 0)$ the origin is globally stable while for $\rho < -9.4$ a non-sliding orbit is present. The transition from a non-sliding to a sliding orbit can be better outlined when the phase-space evolution of the system is investigated on both side of the *sliding bifurcation point*. In particular, as shown in Figs. 2–3, we observed that the fixed point of the switching map corresponding to the non-sliding orbit enters the sliding strip at the bifurcation point and sliding orbits are then generated for further

parameter variations.

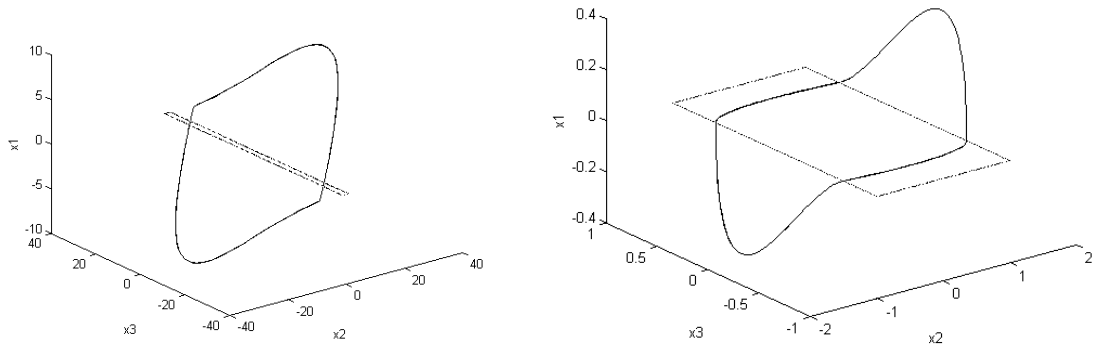


(a) (b)

Figure 2: Phase space diagrams before (a) and after (b) the bifurcation point. The apparent change in size of the sliding strip is due to a mere change of scale.

Using the analytical tools sketched in previous sections, the bifurcation can be located analytically and the theoretical bifurcation point (the parameter value at which the fixed point sits on the boundary of the sliding strip) was found to be $\rho = 2.098841$. This can be done, by imposing the additional condition that the fixed point, corresponding to a non-sliding orbit, belongs to the boundary of the sliding strip onto the system of necessary conditions of existence (14). In doing so, a system of equations defining the location of the bifurcation point as a function of the parameter $\rho$ can be obtained.

After the sliding bifurcation, the sliding orbit contains longer and longer sliding sections until for $\rho = 0$ the origin becomes the only stable attractor. As depicted in Fig. 1, this remains the only equilibrium until at $\rho \approx -9.4$, a new simple limit cycle is generated after a saddle-node bifurcation. Again, using the analytical tools devised above, this bifurcation was located analytically and shown to be a saddle-node bifurcation of the system switching map, characterised by having both the eigenvalues of the map Jacobian crossing the unit circle at $+1$. This bifurcation, actually, generates a pair of equilibria, one stable and the other unstable, hence the existence of a corresponding stable and unstable simple orbits was also detected.

## 6 Multi-Sliding Bifurcations

We now consider $\rho = 1$, fixed to a value at which a sliding orbit exist, and vary the position of the system poles via the parameter $\omega$. In doing so, we seek to uncover possible bifurcations of sliding orbits into more complex dynamical behaviour. Numerical experiments confirm that as $\omega$ is varied, the periodic section of the sliding orbit under investigation undergoes a geometric "twist" that leads to the appearance of an additional sliding section (see Fig. 4(b)). This mechanism is due to the fact that the eigenvalues of the linear part of the system are conjugate complex,

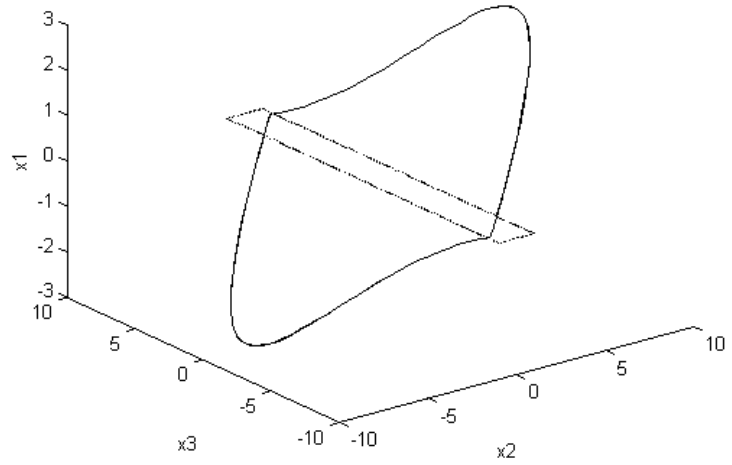


Figure 3: Phase space diagrams of the simple limit cycle at the bifurcation point. It can be clearly seen that the orbit intersects the switching plane on the boundary of the sliding strip

thus causing the onset of oscillating modes corresponding to "twists" of the system solution in the phase space. When this occurs, a bifurcation is observed from a sliding orbit to a periodic solution characterised by two sliding sections, which we term *2-sliding orbit*. We will refer to such a bifurcation as a *multi-sliding bifurcation*.

Further parameter variations will cause a similar bifurcation to occur, so that a 3-sliding solution may be generated from a 2-sliding solution (see Fig. 4(b)) and so on. Specifically, as shown in Fig. 5, a "sliding adding" scenario is observed. Here, a cascade of multi-sliding bifurcations causes the formation of multi-sliding orbits characterised by an increasing number of sliding sections, see Fig. 4. The analysis of this scenario is currently under investigation. There is a fascinating similarity between the bifurcation diagram described above and the so-called "chattering and sticking" behaviour recently observed in mechanical oscillators with impacts [5].

# 7 Chattering Orbits

Sliding orbits are present only for relay feedback systems with linear part having relative degree equal to one. If the relative degree is two, there may be chattering orbits instead. Then, the sliding part of the orbit is replaced by a part with fast switchings [17]. The number of switchings are finite on any bounded time interval, so the chattering is no sliding motion. It can, however, be shown that in some cases the chattering can be replaced by a sliding motion for analysis purposes. This was done in [17] in order to prove that there exists fourth-order transfer functions,

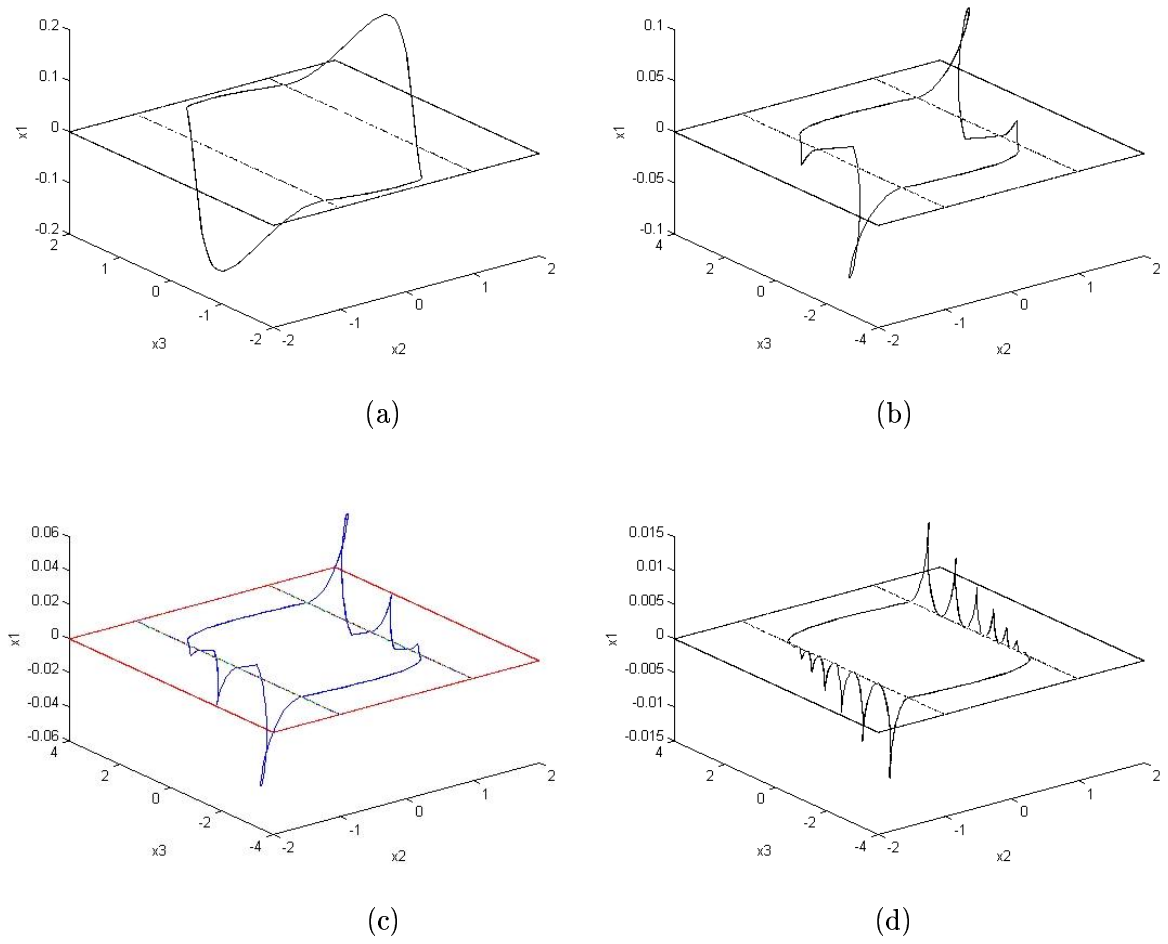


Figure 4: Phase space diagrams of a sliding orbit (a), a 2-sliding (b), a 3-sliding (c) and a 7-sliding (d) ones. Notice the presence of "twists" in the periodic sections of the orbits depicted here.

for example, of the form

$$G(s) = k\frac{(s^2 + 2\sigma\rho s + \rho^2)}{(s^2 + 2\zeta\omega s + \omega^2)(s + \lambda)^2}$$

that gives chattering orbits. The chattering orbits appear when the zeros of $G$ are close to the origin and at least one is in the right half-plane. This corresponds to that the sliding motion is unstable.

Preliminary investigations of fourth-order relay feedback systems show that similar bifurcations as for the sliding orbits are present. It seems, however, as if these bifurcations only describe a subclass of all possible phenomena.

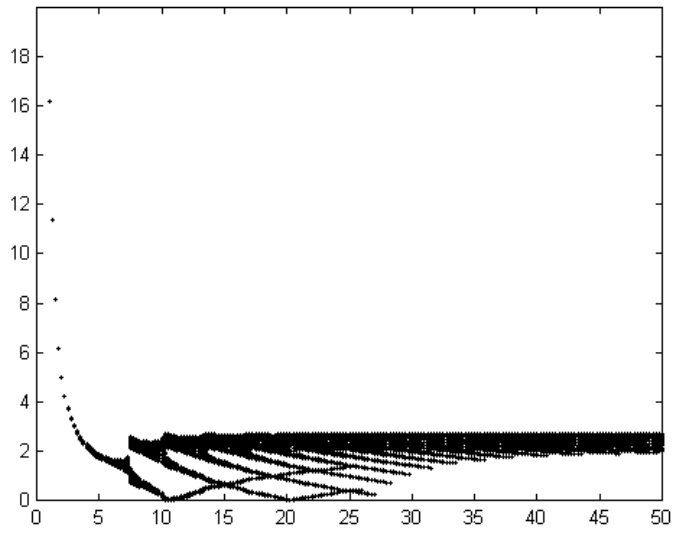


Figure 5: Bifurcation diagram of a sliding orbit showing the second component of the Poincaré map as $\rho$ is kept constant and $\omega$ is varied. Notice the appearance of several fingers corresponding to additional sliding sections (sliding adding scenario). The apparent reflection of some of the fingers is due to the numerical code used.

# 8 Conclusion

We discussed the existence and stability of sliding and non-sliding periodic solutions in a class of relay feedback systems. The occurrence of a novel class of bifurcations was outlined. In particular, a sliding bifurcation was defined as the transition from a simple limit cycle to a sliding orbit. Such a bifurcation has been characterised in terms of the fixed point of an appropriate Poincaré map and has been located analytically in the case of a third-order relay feedback systems. Also, the occurrence of multi-sliding bifurcations causing the metamorphosis of a sliding orbit into more complex dynamical behaviour has been outlined.

We conjecture that the features described in this paper are not specific to relay feedback systems but are instances of a more general class of novel bifurcations in piecewise linear, and more generally, piecewise smooth dynamical systems. This is the subject of on-going research.

Preliminary results indicate that similar sliding bifurcations are the cause of the occurrence of sliding orbits also in applications such as DC/DC converters and friction oscillators [23, 26].

# Acknowledgement

The authors would like to thank Francesca Mazzulla to whom the numerical simulations reported in this paper are mostly due. Mario di Bernardo would like to acknowledge support from the Nuffield Foundation (grant scheme 'NUF-NAL'). The work by Karl Henrik Johansson was

supported by the Swedish Foundation for International Cooperation in Research and Higher Education and by Telefonaktiebolaget L M Ericsson.

## References

[1] A. A. Andronov, S. E. Khaikin, and A. A. Vitt. *Theory of Oscillators.* Pergamon Press, Oxford, 1965.

[2] K. J. Åström. Oscillations in systems with relay feedback. In K. J. Åström, G. C. Goodwin, and P. R. Kumar, editors, *Adaptive Control, Filtering, and Signal Processing*, volume 74 of *IMA Volumes in Mathematics and its Applications*, pages 1–25. Springer-Verlag, 1995.

[3] Karl Johan Åström and Tore Hägglund. Automatic tuning of simple regulators with specifications on phase and amplitude margins. *Automatica*, 20:645–651, 1984.

[4] D. P. Atherton. *Nonlinear Control Engineering: Describing Function Analysis and Design.* Van Nostrand Reinhold Co., London, U.K., 1975.

[5] Chris Budd and Felix Dux. Chattering and related behaviour in impact oscillators. *Phil. Trans. Royal Society London A*, 347:365–389, 1994.

[6] M. di Bernardo, A. R. Champneys, and C. J. Budd. Grazing, skipping and sliding: analysis of the nonsmooth dynamics of the DC/DC buck converter. *Nonlinearity*, 11:858–890, 1998.

[7] M. di Bernardo, E. Fossas, G. Olivar, and F. Vasca. Secondary bifurcations and high periodic orbits in voltage controlled buck converter. *International Journal of Bifurcations and Chaos*, 1997.

[8] M. di Bernardo, F. Garofalo, L. Glielmo, and F. Vasca. Nonlinear phenomena in pulse width modulated feedback controlled systems. *Proceeding CDC96 (International Control and Decision Conference*, 1:2161–2166, 1996.

[9] M. di Bernardo, F. Garofalo, L. Glielmo, and F. Vasca. Switchings, bifurcations and chaos in DC/DC converters. *IEEE Transactions on Circuits and Systems - I: Fundamental Theory and Applications*, 45:133–141, 1998.

[10] S. H. Doole and S. J. Hogan. A piecewise linear suspension bridge model: nonlinear dynamics and orbit continuation. *Dynamics and Stability of Systems*, 11:19–29, 1996.

[11] M. I. Feigin. Doubling of the oscillation period with $c$-bifurcations in piecewise continuous systems. *PMM*, 34:861–869, 1970.

[12] M. I. Feigin. On the generation of sets of subharmonic modes in a piecewise continuous system. *PMM*, 38:810–818, 1974.

[13] A. F. Filippov. *Differential Equations with Discontinuous Righthand Sides.* Kluwer Academic Press, 1988.

[14] I. Flügge-Lotz. *Discontinuous Automatic Control.* Princeton University Press, 1953.

[15] E. Fossas and G. Olivar. Study of chaos in the buck converter. *IEEE Transactions on Circuits and Systems - I: Fundamental Theory and Applications*, 43:13–25, 1996.

[16] S. J. Hogan. On the dynamics of rigid-block motion under harmonic forcing. *Proc. Roy. Soc. London A*, 425:441–476, 1989.

[17] K. H. Johansson, A. Barabanov, and K. J. Åström. Limit cycles with chattering in relay feedback systems. In *Proc. 36th IEEE Conference on Decision and Control*, San Diego, CA, 1997.

[18] K. H. Johansson, A. Rantzer, and K. J. Åström. Fast switches in relay feedback systems. *Automatica*, 35(4), April 1999. To appear.

[19] G.M. Maggio, M. di Bernardo, and M.P. Kennedy. Nonsmooth bifurcations in a PWL model of the colpitts oscillator. *IEEE Transactions on Circuits and Systems I*, 1998.

[20] Yu. L. Neimark. *Methods of pointwise mappings in the theory of nonlinear oscillations.* NAUKA, Moscow, 1972. (In Russian).

[21] L. E. Nusse and J. A. Yorke. Border collision bifurcation: an explanation for observed bifurcation phenomena. *Physical Review E*, 49:1073–1076, 1994.

[22] M. Oestreich, N. Hinrichs, K. Popp, and C. J. Budd. Analytical and experimental investigation of an impact oscillator. *Proceedings of the ASME 16th Biennal Conf. on Mech. Vibrations and Noise*, 1996.

[23] K. Popp, N. Hinrichs, and M. Oestreich. Dynamical behaviour of friction oscillators with simultaneous self and external excitation. *Sadhana (Indian Academy of Sciences)*, 20:627–654, 1995.

[24] Ya. Z. Tsypkin. *Relay Control Systems.* Cambridge University Press, 1984.

[25] V. I. Utkin. *Sliding Modes and Their application in VSS.* Mir Publishers, Moscow, 1978.

[26] D. M. Wolf, M. Verghese, and S. R. Sanders. Bifurcation of power electronic circuits. *Journal of the Franklin Institute*, 331B:957–999, 1996.